

## RESEARCH ARTICLE

# Machine Learning Based Design of Pattern Reconfigurable Antenna

**AHMED M. MONTASER** 

Electrical Engineering Department, Faculty of Technology and Education, Sohag University, Sohag 82524, Egypt


e-mail: Ahmed.Montaser1@techedu.sohag.edu.eg

**ABSTRACT** In this study, a Machine Learning (ML) is implemented to soft computation of the Reconfigurable Horn Bowtie Dumbbell (RHBD) antenna at operating frequency range from 26 GHz to 29.5 GHz for 5G applications. An adaptive learning rate approach is used to build a ML model on a 5-layer system utilizing a simulated database of 180 RHBD antennas. In the training stage of a hybrid method that combines the advantages of particle swarm optimization (PSO) with a modified version of the gravitational search algorithm (MGSA), the architecture frame and hyper-parameters of the ML model are optimized. A precise electromagnetic analysis platform is used to simulate 180 RHBD antennas with varying geometrical properties in terms of the resonant frequency in order to create the database for training and testing the model. The ML model is tested and validated using a fabricated RHBD antenna operating at 27.5 GHz. Then, three PIN diodes are placed in the gaps of the reflectors located at the back of the antenna, and by changing the state of these PIN diodes, it can be noticed that they have a significant and direct effect on the radiation pattern, as they are able to change the beamwidth from  $10.7^\circ$  to  $156.2^\circ$ . The suggested antenna makes it easier to create dynamic radiation patterns that may be utilized to reconfigure the coverage area as required in accordance with the spatial-temporal user and traffic variations in high mobility environments.

**INDEX TERMS** Reconfigurable antenna, neural networks, machine learning, mm-Wave, optimization techniques.

## I. INTRODUCTION

Due to the urgent need to reach more users while maintaining a dependable communication system that satisfies end-user needs, the world recently saw a rapid transition in the wireless communication business. As a consequence, a number of contemporary standards and applications have been developed, including fifth generation (5G) communications, big data applications, the internet of things (IoT), and vehicular communications, etc. [1]. These new technologies are, however, creating new problems for radio frequency congestion and have crossed wireless frequency band allotment. To meet these issues, the phenomena of antenna reconfigurability has emerged [2] because to its promising properties of tailoring the operating frequency and beam width management for the intended applications.

The associate editor coordinating the review of this manuscript and approving it for publication was Filbert Juwono .

Reconfigurable antennas (RAs) that have the ability to dynamically change their characteristics, such as their radiation pattern, operational frequency, and polarization, have drawn a lot of interest [3], [4], [5], [6], [7], [8], [9]. In specifically, the reconfigurable antennas with radiation pattern reconfigurability aid in enhancing system performance [10], energy efficiency, and communication security by directing signals in the desired directions while minimizing interference in the unwanted directions [11].

In addition to the properties that allow for reconfiguration, antenna compactness is highly valued since miniature antennas drastically reduce the dimensions of electronic systems [12]. The antennas are therefore ideal for contemporary communication systems and gadgets because of their reconfigurability and compactness. Various thin, small, reconfigurable single-band, multi-band antennas [13], [14]. Modern technologies, however, require compactness in a single antenna, functioning at many frequency ranges, reliable band switching, and control over beam width [15].

The aforementioned antennas' potential applications may therefore be constrained. The distribution or configuration of electric or magnetic current on an antenna's construction can be changed to change the radiation pattern that is emitted by the antenna. Another way to achieve pattern reconfigurability without significantly changing the operating frequency is to establish linkages between source currents and the antenna's radiation pattern. Changes in working frequency can be avoided while still obtaining radiation pattern reconfigurability by using a tunable circuit or some particular antenna types (such as parasitically coupled antennas or reflector antennas) [16], [17], [18], [19].

The following are a few techniques that have been discovered to accomplish radiation pattern reconfigurability:

- **Changes in structure or mechanics:** It has been demonstrated that altering the reflective surface of a reflector antenna physically by separating it from its excited point can vary the radiation pattern while maintaining the operational frequency. One use of this is to modify an antenna's reflector structure to produce a reshaped beam and then incorporate a motor or actuator to provide automatic radiation pattern reconfiguration.
- **Electrical modifications:** It has been discovered that it is possible to modify the structure of the antenna in order to vary its radiation pattern. An application of this is the ringed slot antenna, which modifies the nulls of its radiation interference pattern by placing PIN diodes around its slot.
- **Parasitic Tuning:** The employment of parasitic elements in an antenna is a very efficient way to achieve the capacity to change the radiation pattern. In order to alter source currents on the antenna surface and hence tilt or steer the antenna beam, they take advantage of mutual coupling phenomena between the driving and tuned antenna elements.

Another area of research focuses on the incorporation of Machine Learning (ML) techniques into an optimization method that selects the ideal antenna characteristics and performance [20], [21], [22], [23], [24]. ML is an effective method for estimating or predicting that has the advantage of learning and may provide accurate results for a given task. Therefore, instead of spending money on expensive simulation and measurement, the recommended DNN model is a trustworthy and accurate computing approach. With regards to the development and optimization of antennas using deep learning, [20] provides a complete study of multiple research articles. It covers the various techniques and algorithms used to generate antenna parameters based on necessary radiation qualities and other antenna requirements. A complicated antenna with high radiation properties was constructed by the authors in [21] using a hybrid DNN system and MGSA-PSO algorithm. An array of 16 antenna elements was constructed, and the DNN system was used to feed the 16 antenna elements in order to achieve the necessary beam-steering.

In [22], the authors used the DNN system and extremely potent algorithms to design a beam steering for a 64 element

plasmonic nano antenna array, as a result, the authors were able to manage all antennas and achieve high precision beam steering. After that, they only used 5 active antennas to make beam steering. The authors of [23] constructed an applicator with 35 antennas that utilizes a multi-resonance technology. This array's design utilized a DNN approach, which significantly aided in the heating of all kinds and sizes of breast cancers. In order to create the radiation patterns, the authors of [24] used a patch antenna array  $4 \times 1$  with an inter-element spacing of  $0.28 \lambda$ . Building a DNN allowed us to obtain the outputs, which were the amplitude and phase of the antenna elements, from the radiation pattern, which served as the input. A number of radiation pattern samples that demonstrate reasonable competence in creating the radiation patterns were used to train the recommended ML. Antennas are typically regarded as the greatest potential candidates for ML s because to the inherent nonlinearities related to their radiation patterns. Given their ability to connect data with actual specialist expertise about problems, as well as their precise and rapid learning and powerful generalization abilities, neural systems are unquestionably widespread.

In this paper, a ML -based model is optimized in the training phase of a hybrid MGSA-PSO algorithm for the resonant frequency computation of the RHBD antenna. The accuracy of the model is further validated on a measured RHBD antenna resonating at 27.5 GHz. The RHBD antenna presented in this work is capable of beamwidth control while requiring a small number of PIN diodes, where only three PIN diodes are used. This RHBD antenna can control 3-dB beamwidths in three planes. The presented paper is organized as follows: In section II, the RHBD antenna design configuration is presented. Section III presents a brief introduction about ML modelling and training. In section IV, discussion, validation and testing the ML model results are explained. The antenna ability of the reconfigurability and beam-width control is presented in the section V. Finally, section VI concludes the results.

## II. DESIGN OF RHBD ANTENNA

This section presents the design structure of the proposed RHBD antenna. This antenna consists of five main parts, which are Substrate Integrated Waveguide (SIW) horn antenna, slotted bowtie antenna, sectoral horn with four arcs director, three half circle reflectors and circular head dumb-bell Defected in Ground plane Structure (DGS) as shown in Fig. 1.

All these parts are installed on the substrate, while the antenna is fed with coaxial cable 50 ohm by SMA connector 2.92mm, 0Hz to 40GHz, 50 Ohm, Solder ST SMD F, and code (SF1521- 60070) installed at the bottom of the antenna. Below is a detailed explanation of each part of the proposed antenna. The first part of the antenna is SIW horn antenna, sectoral horn antenna are integrated by using the same single substrate based on the SIW technology. As a result they are easy to fabricate and the structure is compact. So the directivity is directed along the x-axis, and it also improves

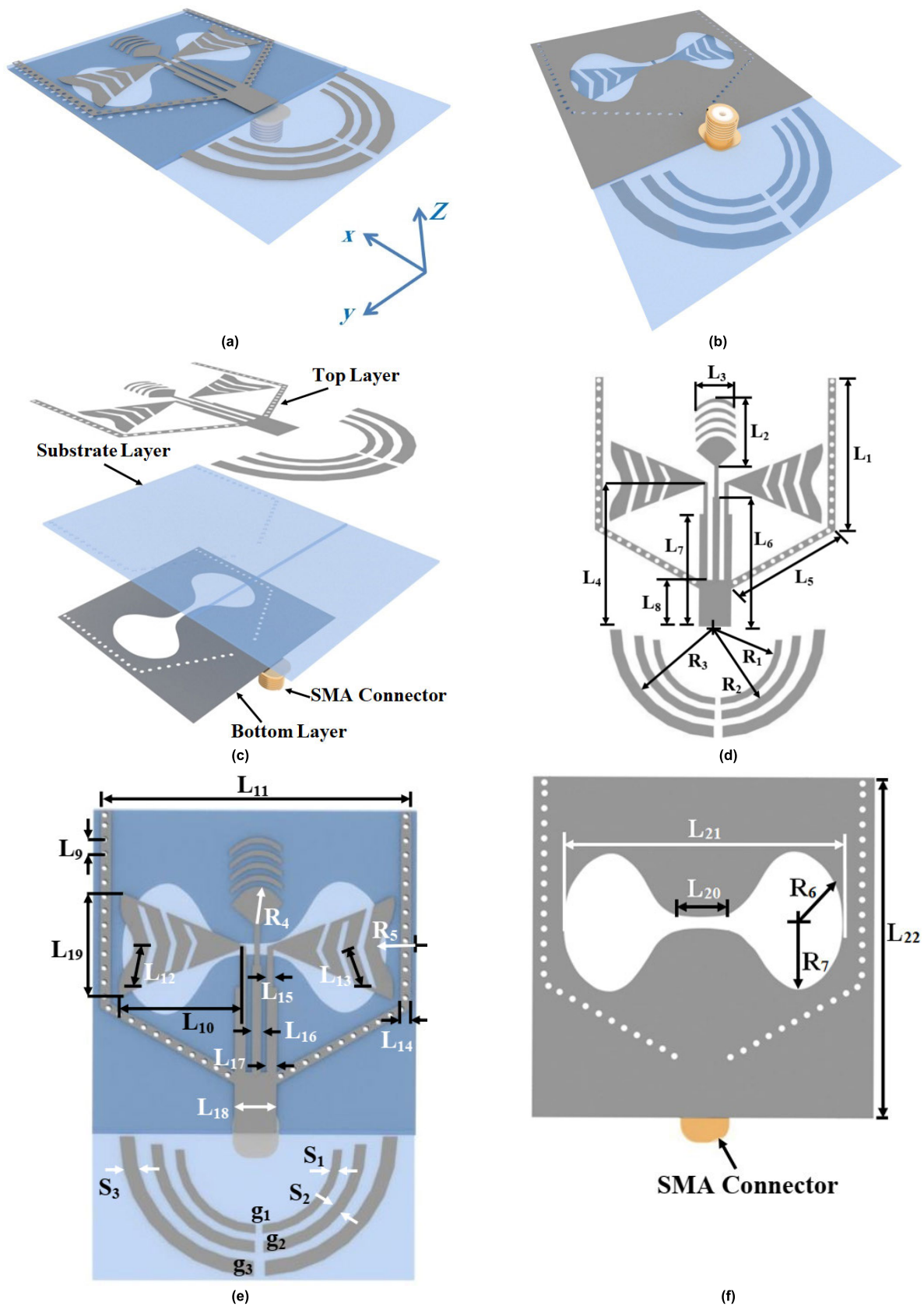


**FIGURE 1.** Proposed antenna structure (a) 3D top view, (b) 3D bottom view, (c) Separated layers for antenna, (d) Top layer with dimension, (e) Top layer with dimension Cont., and (f) Bottom layer with dimension.

the reflection coefficient matching for RHBD antenna. Also, SIW horn antenna has high gain and narrow beam-width under conditions. As for the second part is slotted bowtie antenna, which is two triangles opposite the head that are fed by a microstrip feed line, and there are opposite slots in the two triangles in order to change the distribution of current inside the antenna from one scenario to another and prevent the occurrence of eddy currents, and it also increases the metallization area of the antenna, and shaping the two wings appropriately which in turn increases the radiation efficiency of the RHBD antenna. Providing three slots on bowtie antenna has a huge advantage because it allows the

creation of a small, compact, low profile antenna with excellent performance such as, for example, a high gain, a changeable radiation pattern, etc. Designing such a bow-tie antenna is very difficult. The physical shape, the number of slots, and their position are critical parameters and must be designed with extreme care and precision.

The third part is the antenna, which is sectoral horn with four arcs director, it is fed by the tape, and plays a key role in directing the radiation and distributing the current in the antenna. On the other hand, when the arcs director is added to the structure, the arcs director pulled the electromagnetic radiation along its main lobe axis. Consequently, the side lobes are decreased, and the directivity is enhanced. Also, the electric field is not only confined seat metal bow but also is concentrated around the arcs director. Therefore, the performance of the RHBD antenna is improved in terms of the gain and directivity. Moreover, the radiation efficiency of the design is enhanced. It may be seen that the directors enhance the radiated power in the transmitter terminal. This results in reducing the losses over the distance and increases the transmitted power in the receiver terminal.

As for the fourth part, which is three included arcs, each arc is a half circle in the middle of each arc, which has a slot; this slot is suitable for placing a diode in it. These reflectors work on the reflection the entire energy in the direction of the radiation pattern, increasing the modes of radiation, increasing the resonance frequencies, modifying the antenna geometry and variation the surface current distribution area. As for the fifth and final part, which is circular head dumbbell defected in DGS, it is a hole drilled in the ground plane for the antenna in the form of a circular head dumbbell, and it works on slower phase variation behavior beyond the resonant frequency, which leads to significantly enhancement the gain and matching the antenna and balancing the current distribution throughout the antenna structure.

### III. MACHINE LEARNING(ML): MODELLING AND TRAINING

Deep learning differs from machine learning by merging functionality collection and regression / classification, containing more neurons, processing synchronously on several layers, naturally extracting features, and validating the best network hyperparameters. The ML system evaluates the input by passing it through the neurons in the multi-layered

pyramid, and the evaluated data is then transmitted to the subsequent layers, enabling the creation of a learning model that is more practical.

In order to determine what the dimensions of the antenna are, which have a strong influence on the antenna characteristics, such as the reflection coefficient and the realized gain, thus, these dimensions are considered input variables for the ML model, and then it is necessary to do the parameters sweep on all antenna dimensions, and from the above, it was found that the most important dimensions are  $L_2$ ,  $L_{11}$ ,  $L_{19}$  and  $L_{21}$ .

Then it can be made clear to us that the sectoral horn with four arcs director length  $L_2$ , the width of the SIW horn antenna  $L_{11}$ , the slotted bowtie antenna length  $L_{19}$  and the circular head dumbbell defected in DGS length  $L_{21}$ . The change in them affect the reflection coefficient greatly, and the greater the length of the variable, the lower the resonance frequency at which the antenna operates as shown in Fig. 2. Also, Table 1 listed the initial, optimized, and decision spaces for each dimension in the proposed antenna.

In a brief explanation of the ML model that is applied to the RHBD antenna and Multilayer perceptrons (MLPs) [25], [26], [27], which, in this inquiry, are preferred because they have been effectively and regularly used in engineering applications. The MLP can be trained using a variety of different techniques, including Levenberg-Marquardt (LM), back propagation, and delta-bar-delta. The MGSA-PSO algorithm [28], [29], which has rapid learning and excellent convergence capabilities, is used in this study to train MLPs. The MLP contains five levels, including an input layer, an output layer, and three hidden layers, as seen in Fig. 3.

The layer's neurons just serve as buffers to distribute the input signals  $\mathbf{x}_i$  to the hidden layer's neurons. After weighing their input signals  $\mathbf{x}_i$  according to the intensities of the relevant input layer connections  $\omega_{ji}$ , each hidden layer neuron  $j$  adds the signals and computes its output  $y_j$  as a function  $f$  of the sum, i.e.

$$y_j = f\left(\sum \omega_{ji}x_i\right) \quad (1)$$

where  $f(\cdot)$  can be a simple threshold function, a sigmoid, hyperbolic tangent, a radial basis function, a purelin function, etc. [26], [27]. The output of the neurons in the output layer is calculated similarly. One of the learning methods that are accessible is employed to modify the weights of the network during training.

The learning algorithm provides the variation in weight of a relationship between neurons  $i$  and  $j$  at time  $t$  as  $\Delta\omega_{ji}(t)$ . Using the formula below, the weights for the LM learning algorithm are updated.

$$\omega_{ji}(t+1) = \omega_{ji}(t) - \Delta\omega_{ji}(t) \quad (2)$$

$$\Delta\omega_{ji} = [\mathbf{J}^T(\omega)\mathbf{J}(\omega) + \mu\mathbf{I}]^{-1}\mathbf{J}^T(\omega)\mathbf{E}(\omega) \quad (3)$$

where the Jacobian matrix, a constant, the error function, and the identity matrix are, in that order,  $\mu$ ,  $\mathbf{E}(\omega)$ , and  $\mathbf{I}$ . The first



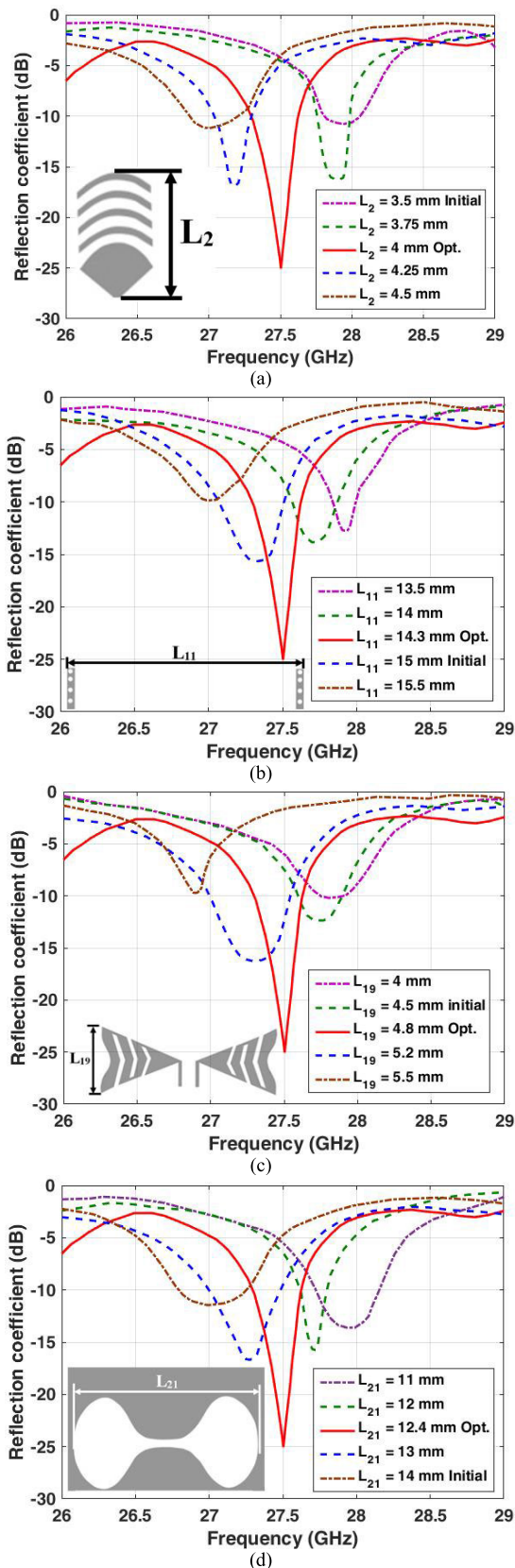


FIGURE 2. Parameters sweep for main dimensions' effects on the reflection coefficient.

TABLE 1. The initial, decision space, and optimized dimensions for proposed antenna. (All unit in mm).

Variable	Initial Value	Decision Space		Best Value
		From	To	
$L_1$	7	6	11	9
$L_2$	3.5	3	5.5	4
$L_3$	3	2	3.5	2.5
$L_4$	9	8.5	9.5	8.7
$L_5$	8.5	6.5	9	7
$L_6$	9	7.5	9.5	7.8
$L_7$	6.5	6	7	6.8
$L_8$	2.5	2	3	2.8
$L_9$	0.8	0.5	1	0.7
$L_{10}$	5.3	5	6	5.6
$L_{11}$	15	13.5	15.5	14.3
$L_{12}$	2.2	2	2.5	2
$L_{13}$	1.5	1.5	2	1.9
$L_{14}$	0.5	0.3	0.5	0.4
$L_{15}$	0.2	0.1	0.4	0.3
$L_{16}$	0.3	0.1	0.4	0.4
$L_{17}$	0.4	0.3	0.6	0.5
$L_{18}$	1.7	1.5	2.5	2
$L_{19}$	4.5	4	5.5	4.8
$L_{20}$	2.5	2	3	2.3
$L_{21}$	14	11	14.5	12.4
$L_{22}$	17	14	18	15
$R_1$	4.5	4	4.8	4.2
$R_2$	5.5	5	6	5
$R_3$	6.5	6	7	6.1
$R_4$	1.5	1.3	2	1.8
$R_5$	1.4	1.3	2	1.8
$R_6$	2.5	2.3	3	2.4
$R_7$	2.8	2.5	3.5	3
$S_1$	0.3	0.3	0.4	0.35
$S_2$	0.45	0.4	0.55	0.5
$S_3$	0.55	0.5	0.65	0.6
$g_1$	0.25	0.25	0.35	0.3
$g_2$	0.4	0.35	0.45	0.4
$g_3$	0.55	0.45	0.55	0.5

variations of the errors with regard to weights and biases are contained in the Jacobian matrix. The value of decreases after each succeeding step and is only raised when a step would raise the total of squares of errors. In this study, a ML model with five different layers input layer, three hidden layers, and the output layer was used. The training technique consists of 180 epochs.

Additionally, the tangent sigmoid, tangent sigmoid, and purelin functions were utilized in the input layer, hidden layer, and output layer, respectively.

The CST-MWS [30] 3D EM solver executing FIT is used to simulate 180 RHDBs with varying geometrical variables in order to create a database for modelling the ML. In Fig. 4, the variables of the simulated RHDBs are topologically depicted.

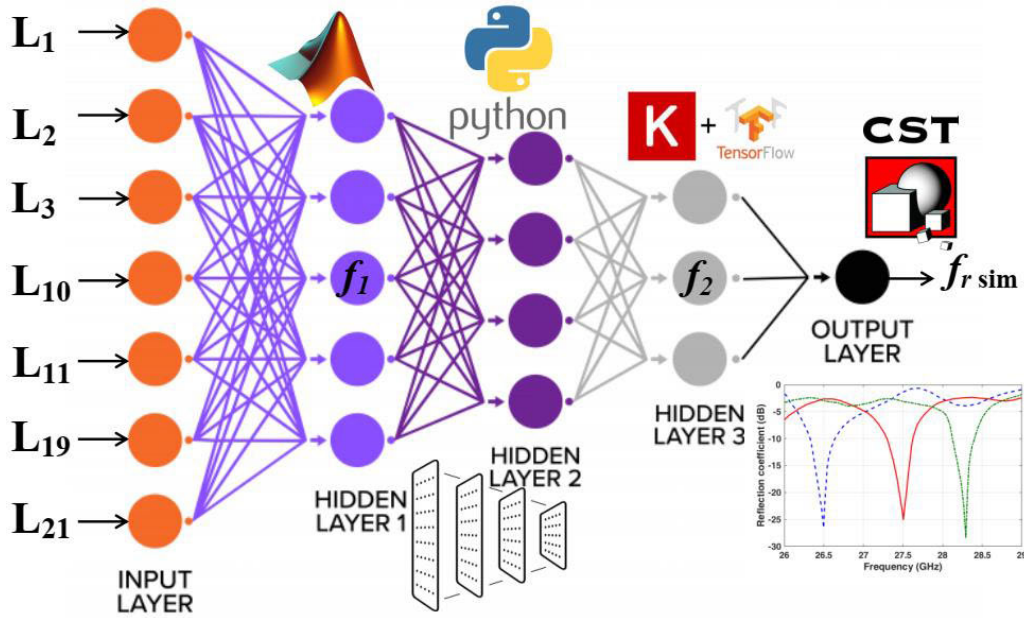


FIGURE 3. The proposed 5-layer ML framework.

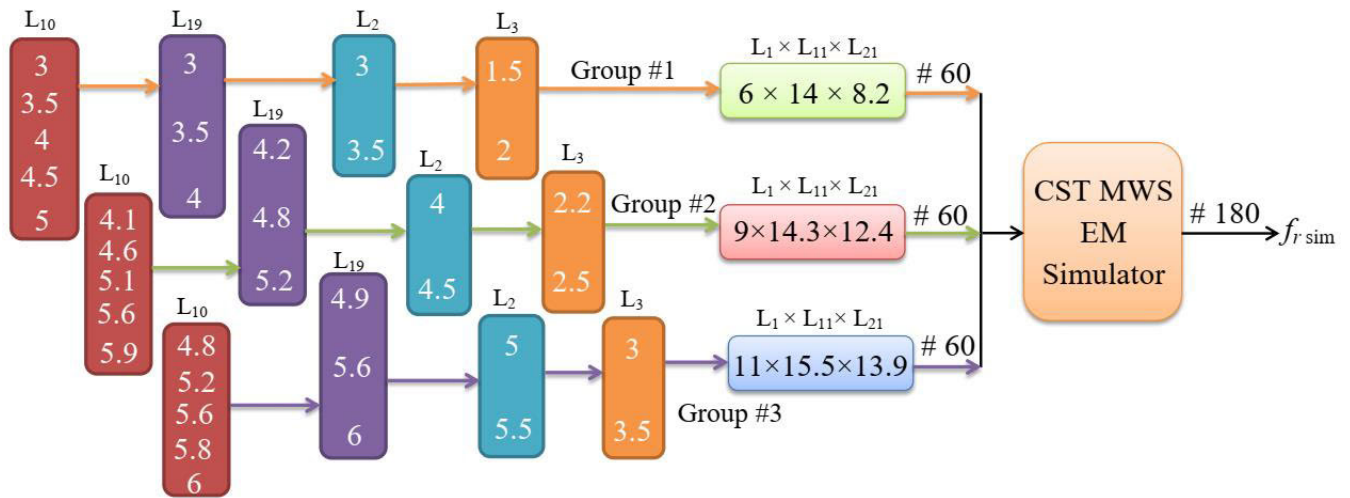


FIGURE 4. Topological illustration of the geometrical parameters of the simulated 180 RHBD antennas by CST 3D EM (dimension unit: mm).

Three groups of antenna parameters are taken into consideration. Each group includes the ground plane slot length and sectoral SIW horn antenna parameters  $L_1 \times L_{11} \times L_{21}$  mm,  $6 \times 14 \times 8.2$  mm,  $9 \times 14.3 \times 12.4$  mm, and  $11 \times 15.5 \times 13.9$  mm. Each group has 60 RHDBs that comprise a parameter combination of  $L_1 \times L_{11} \times L_{21}$ . E. g. for the first group of  $6 \times 14 \times 8.2$  mm, there are 60 RHDBs including the parameter combination of  $(L_{10}: 3, 3.5, 4, 4.5, 5 \text{ mm}) \times (L_{19}: 3, 3.5, 4 \text{ mm}) \times (L_2: 3, 3.5 \text{ mm}) \times (L_3: 1.5, 2 \text{ mm})$ . CST package provides the simulated resonance frequency  $f_r$  of each RHBD antenna with a specific antenna parameter.

The simulated resonant frequency changes versus antenna number are depicted in Fig. 5. While the sectoral SIW horn

antenna and ground plane slot dimensions both affect the resonant frequency, the relationship between the antenna parameters and the resonant frequencies is therefore very nonlinear. The simulations are performed at the frequency range from 26 to 29.5 GHz by 180 points.

Of the three groups that the ML model trains on, it is clear to us that each group has a dominant frequency of the mm-wave frequencies, the rest of the frequencies resonant around it. For example, in first group, its dominant frequency range is 26 to 27 GHz, and the all frequencies of this group resonant in this frequency range. As for the second group, its dominant frequency range is 27 to 28 GHz, and the third and last group, its dominant frequency range is 28 to 29.5 GHz, and all

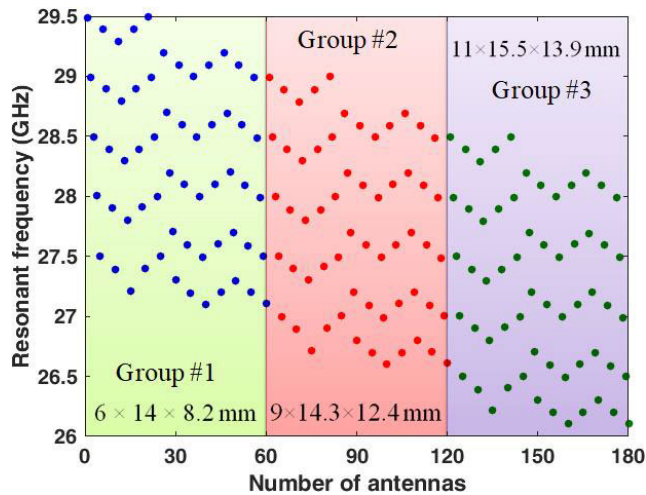


FIGURE 5. Simulated resonant frequency variation for each antenna group defined in Fig. 4.

these three frequencies ranges belong to the dominant mm-wave frequencies. Fig. 6 shows three dominant frequencies from these ranges, Fig. 6a illustrates reflection coefficient for the dominant frequencies, and Figs 6b, 6c, and 6d have shown the horizontal and vertical radiation pattern at each of the frequencies 26.5 GHz from the third group, 27.5 GHz from the second group, and 28.3 GHz from the first group, respectively.

IV. VALIDATING AND TESTING THE ML MODEL

In this section, the simulation and measurement results of the training RHDB antenna will be presented and analyzed. The ML model with three layers was trained to generate the resonant frequency for each group of antenna parameters based on the association between the input and the goal. The ML model was tested using 18 RHBD antennas, whereas 162 RHBD antennas were utilized for training. The scatter diagrams of the computed and simulated resonant frequency results for the training and testing datasets are provided in Fig. 7 to visually identify the connections between the results.

The ML model has calculated the average percentage errors (APE) for the resonant frequencies, as shown in Fig. 8 [31]. It is obvious that for every deep learning application, the amount of training points assigned has an impact on the APE value. In contrast, increasing the amount of training points enhances the system’s precision, and vice versa. A suitable APE of 0.316% was achieved as for the 180 RHBD antennas training data on the basis of Fig. 8, which depicts the topology of computing the APE for CST models. It is obvious that the points will reflect a linear pattern, indicating that the results have a strong linear association.

The RHBD antenna variables that weren’t used throughout the training stage were used to further explore the validity of the current technique, operating from 26 to 29.5 GHz was designed via CST and then fabricated on the Rogers® Duroid™ RT5880 with a 0.508 mm substrate

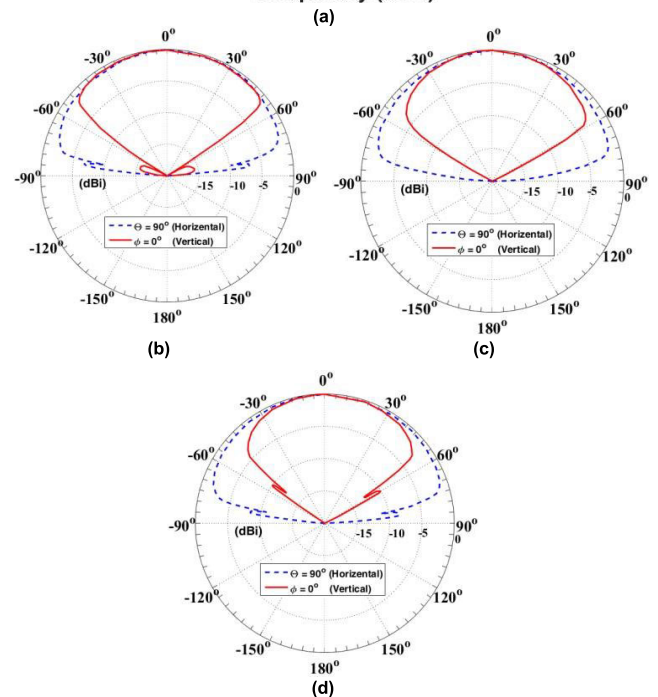
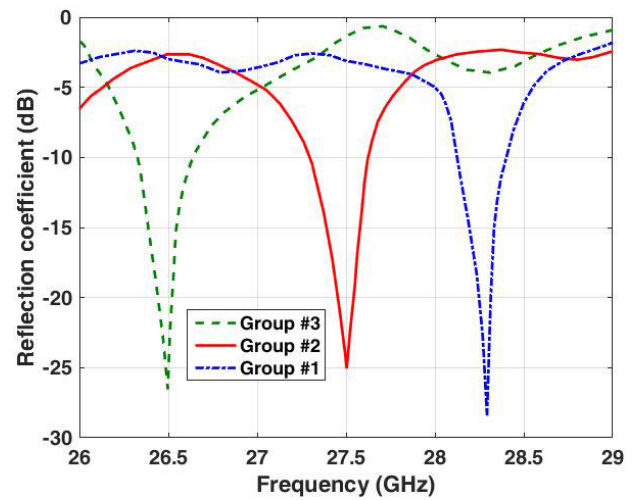


FIGURE 6. Three dominant frequencies for training groups. (a) Reflection coefficient for the dominant frequencies, (b), (c), (d) horizontal and vertical radiation pattern for the dominant frequencies 26.5, 27.5 and 28.3 GHz, respectively.

thickness, relative permittivity  $\epsilon_r=2.2$ , and loss tangent  $\tan\delta =0.0009$  substrate.

Table 1 showed the corresponding antenna dimensions. A good match between the measured and simulated for reflection coefficient  $S_{11}$  results is seen in Fig. 9 (a). The antenna can accomplish a good agreement at operating frequency 27.5 GHz with a realized gain of 8.43 dBi, as illustrated in Fig. 9 (b).

V. RECONFIGURABILITY AND BEAM-WIDTH CONTROL

In the previous sections, the ability of the proposed antenna to operate at any frequency in the range from 26 to 29.5 GHz is explained depending on the amount of change in the antenna



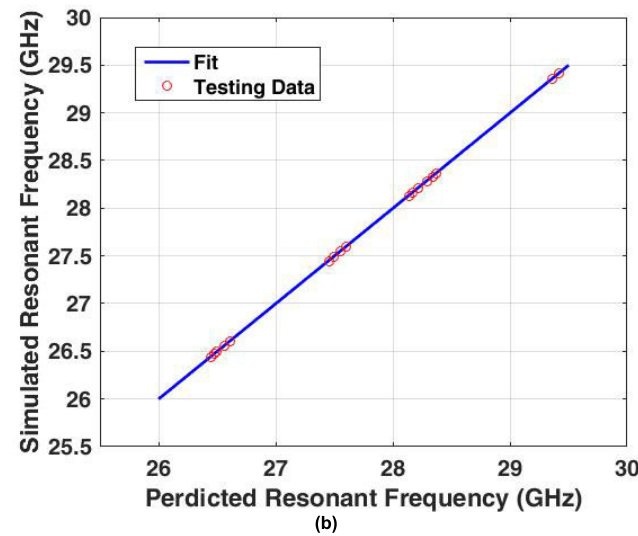
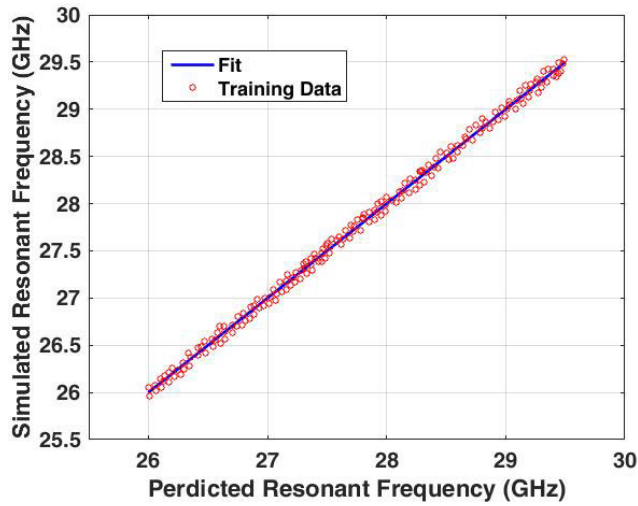


FIGURE 7. Scatter diagrams of the simulated and computed resonant frequency values by the ML model for (a) Training data, (b) Test data.

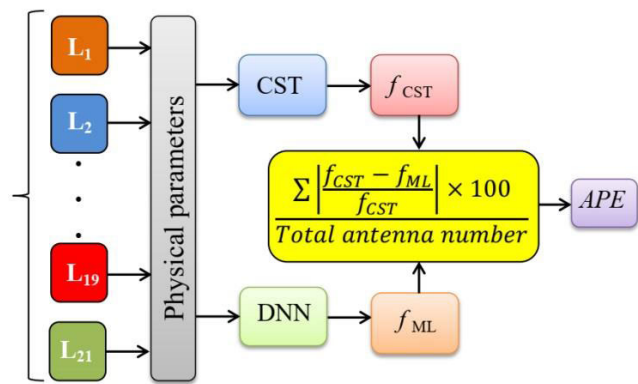


FIGURE 8. The topology of the calculating APE for CST models.

dimensions. In this section, the effect of changing the state of the three PIN diodes  $D_1$ ,  $D_2$  and  $D_3$  in the gaps  $g_1$ ,  $g_2$  and  $g_3$  is studied; these gaps are located in the middle of the

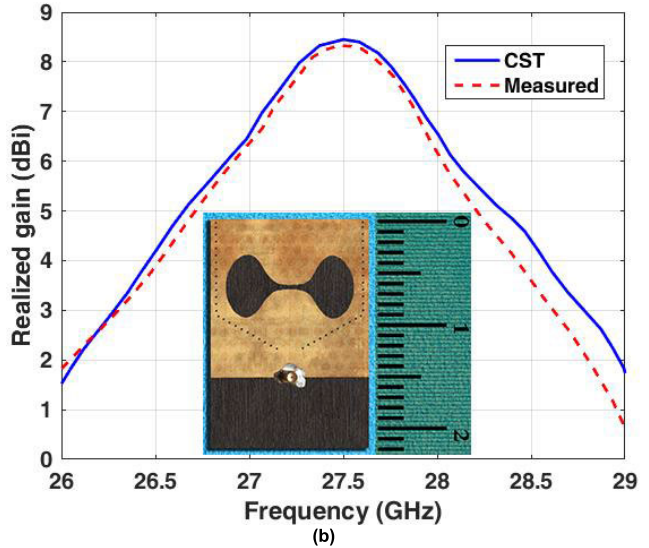
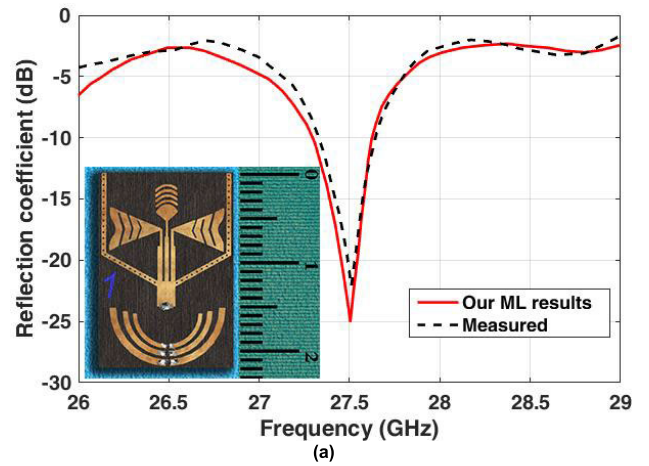


FIGURE 9. Antenna radiation characteristics, (a) Reflection coefficient, (b) Realized gain. The inset figure illustrates the front and back view of fabricated antenna.

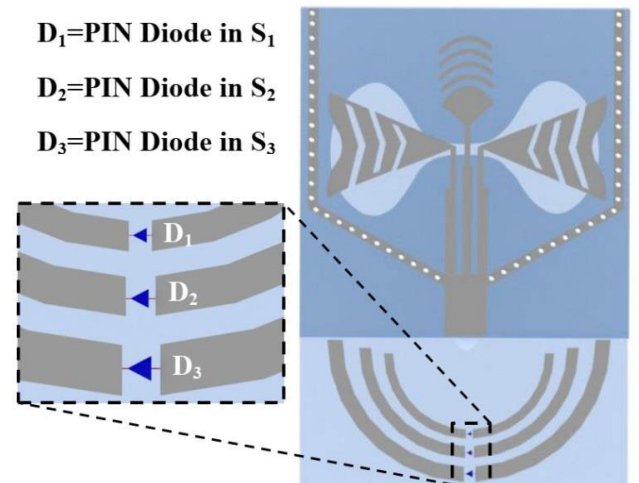
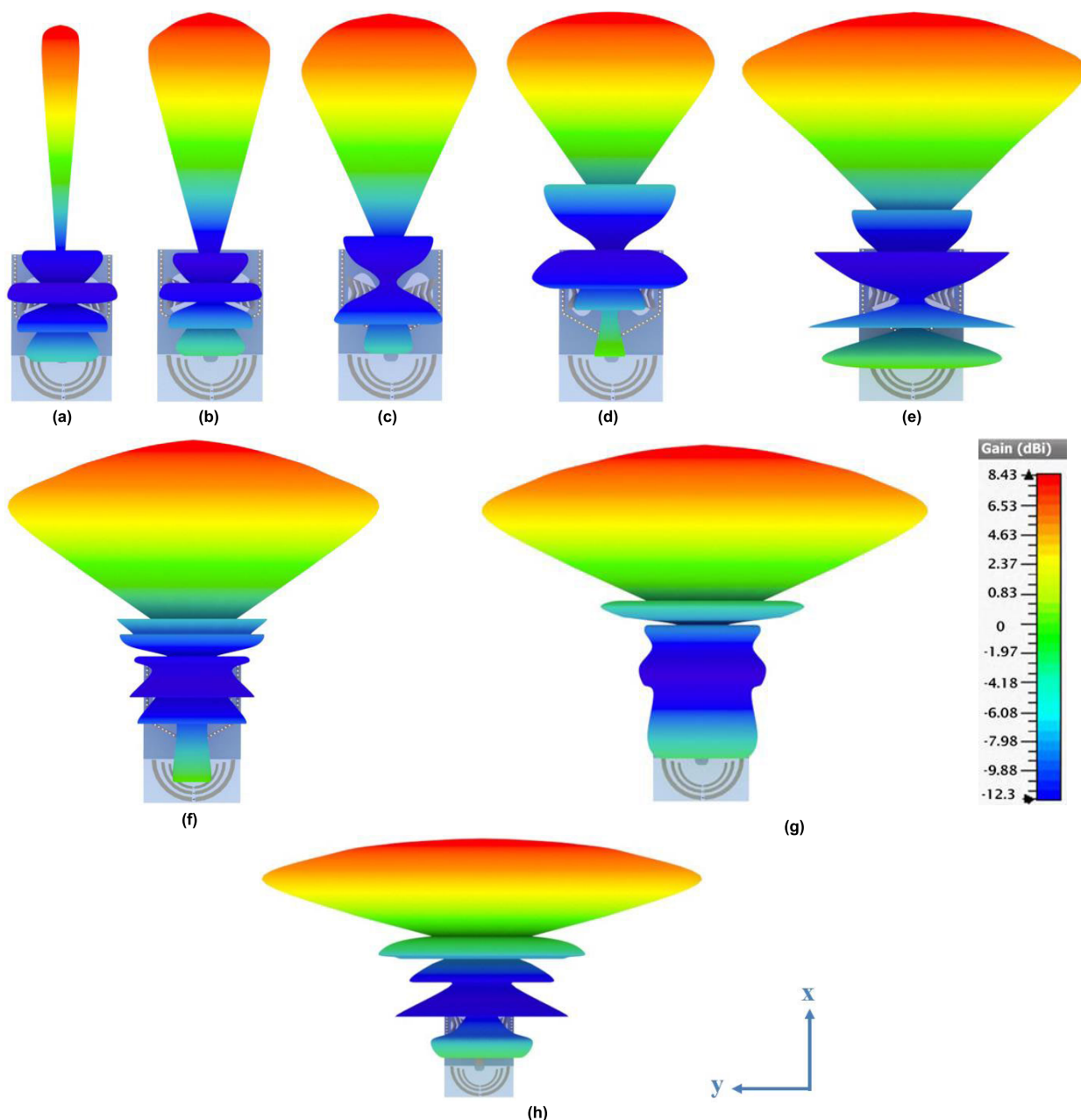


FIGURE 10. The proposed antenna after connecting three PIN diodes.

three half circle reflectors at the back of the antenna, as shown in Fig. 10. Placing these PIN diodes in those gaps changes





**FIGURE 11.** 3D radiation pattern for all scenarios are listed in Table 2. (a) Sc. #8, (b) Sc. #7, (c) Sc. #6, (d) Sc. #5, (e) Sc. #4, (f) Sc. #3, (g) Sc. #2, (h) Sc. #1.

the path of the current distribution in the antenna, which in turn changes the beam width of the radiation beam out of the antenna. Therefore, all cases resulting from changing the state of the three PIN diodes and the consequent change in the beam width radiation out of the antenna have been clarified, as listed in Table 2.

As a result of each state of the PIN diodes, it can be noticed that the beam width changes with changing the state of the PIN diodes from  $10.7^\circ$  to  $156.2^\circ$ . For example, in case of the first scenario, when all the PIN diodes are OFF state, the beam width equal to  $156.2^\circ$ , and in the case of the eighth scenario,

the state of all the PIN diodes are ON state, the beam width equal to  $10.7^\circ$  as shown in Fig. 11.

Table 2 clearly shows that the smaller the HPBW for the antenna beam, the greater the antenna gain, as seen in scenario 8, where the beam out coming from the antenna was as narrow as possible,  $10.7^\circ$ , and the gain was 9.75 dBi, and scenario 1, when the antenna’s beam out was as wide as possible,  $156.2^\circ$ , and the gain was 6.91 dBi, that is, the difference between the largest beam and the smallest beam is 2.84 dBi. That is, it is approximately equal to 3 dB, implying that the antenna almost lost half of its gain, which is a significant loss

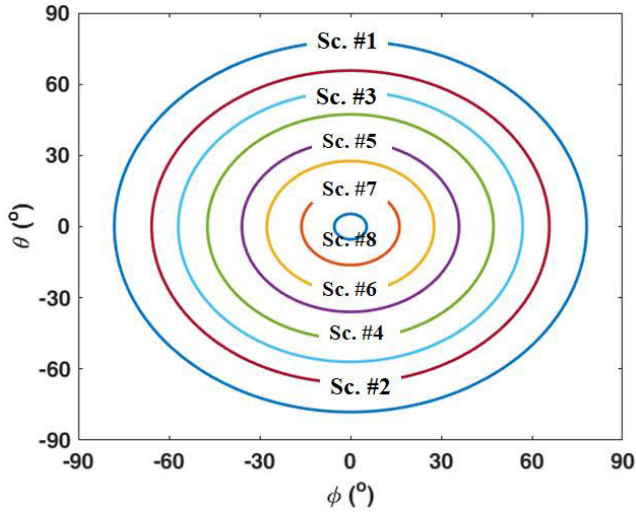


FIGURE 12. Simulated  $-3$  dB contour patterns of the RHBD antenna for each case in Table 2.

value for a single antenna, to change its beamwidth from a small to a large one, and this is considered an advantage of designing this antenna, that it can control the beamwidth of the outgoing beam without losing more than half of its power. Because if any antenna loses more than half of its power, its coverage in the case of a wide beam will be weak and its range will be small. However, because it contains the SIW horn antenna and the sectoral horn antenna with four arcs director, this antenna has a high gain and directivity does not exceed half its power loss, and its coverage and range are strong.

To confirm the clarification of the RHBD antenna coverage area in each of the scenarios mentioned in the Table 2, Fig. 12 illustrates the simulations  $-3$  dB contour patterns for illustrating the angular coverage of all the RHBD antenna scenarios. From this it becomes clear the amount of change in the beamwidth at  $-3$  dB HBPW of the output antenna beam from  $10.7^\circ$  to  $156.2^\circ$ .

In order to validate the radiation pattern results in each scenario in Table 2, the simulated radiation pattern results were compared with the measurements results for the same scenarios. Fig. 13 shows a comparison between simulation and measurement results for scenarios 1 and 8. Considering that Sc. #1 is the largest beamwidth coming out of the antenna, which is  $156.2^\circ$ , and Sc. #8 is the smallest beamwidth coming out of the antenna, which is  $10.7^\circ$ , the results show that there is an excellent agreement between the simulation results and the measurements. Hence, we conclude that based on changing the states of the PIN diodes in the proposed antenna, the current distribution changes in all parts of the antenna, resulting in a change in the beam width of the radiation beam out of the antenna, and then this antenna can be used in many applications such as dynamic radiation patterns that may be utilized to reconfigure the coverage area as required in accordance with the spatial-temporal user and traffic variations in high mobility environments.

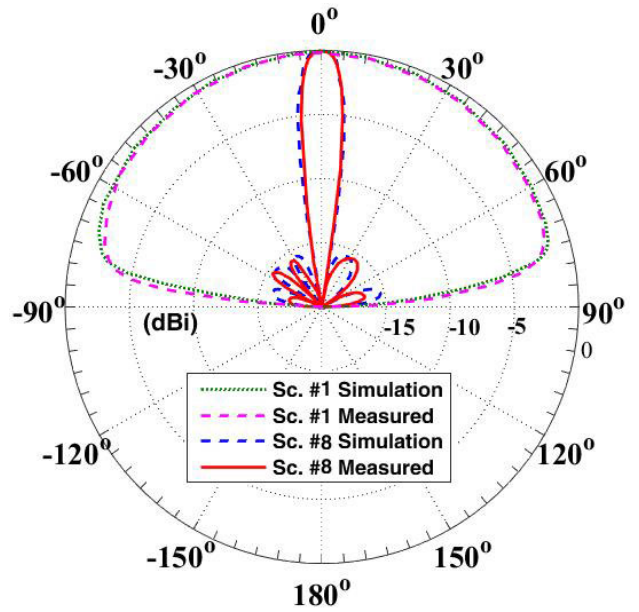


FIGURE 13. A comparison between simulation and measurement normalized gain results for Sc. #1 and Sc. #8.

The basic idea of our proposed antenna is that it controls the angle of the beamwidth coming out of the antenna, or, in other words, the angle of the coverage area covered by the antenna. Either the coverage angle is small enough to extend the wireless network service to only one person, for example, without interference with other networks and frequencies in the work area. Either the angle is large enough to extend the wireless service to a large number of individuals, or between the coverage of one individual and a large number of individuals, the angle of coverage varies according to the exact area to be covered.

This is a reconfigurable system for covering the required area of the work space, and this is considered a great and distinctive control over the required coverage. There are also some other antennas that have some simple control over the pattern and are reconfigurable, but depend on a complete change in the form of radiation from omnidirectional to bidirectional or endfire, but they do not give complete control over the angle of coverage of the work space. There are a number of these antennas that have been compared to our proposed antenna in Table 3. The power of controlling the coverage angle in our proposed antenna is due to the hybrid RHBD antennas, that is, several antennas mixed together by the optimization technique in a way that makes them control more flexibly the degree of coverage of the work space.

A comparison of the most recently reported reconfigurable antenna types described in the literature is given in Table 3. Fundamental properties in terms of antenna type, type of reconfiguration, number of switches used, frequency of operation, and total size of the antennas, beamwidth range controller, average realized gain, maximum radiation efficiency and the control algorithm are provided and have been

TABLE 2. Antenna properties at each PIN diode states.

Sc. # no.	PIN diodes states			HPBW (°)	Gain (dBi)	Radiation efficiency %
	D <sub>1</sub>	D <sub>2</sub>	D <sub>3</sub>			
1	OFF	OFF	OFF	156.2	6.91	65.9
2	OFF	OFF	ON	131.5	7.25	69.2
3	OFF	ON	OFF	113.9	7.58	73.6
4	ON	OFF	OFF	94.6	7.89	77.4
5	ON	ON	OFF	71.8	8.32	81.3
6	ON	OFF	ON	55.3	8.77	85.1
7	OFF	ON	ON	32.4	9.28	89.7
8	ON	ON	ON	10.7	9.75	93.2

TABLE 3. Comparison between the proposed antenna and other reported reconfigurable antennas.

Ref.	Topology	Reconfigur. Type	Frequency and No. of bands (GHz)	Beam width range controller	No. of S.W.	Antenna size (mm)	Avg. Gain (dBi)	Max. Eff. (%)	Control algorithm
[20]	Multiple structures	Frequency	1-7 5 & 6 bands	No control	3	84 × 64	3.65	NA	Regression trees
[37]	tortoise-shaped patch	Frequency	2.45 - 13.7 3 band	No control	1	33 × 22	3.19	94.02	NodeMCU
[38]	Array 3 × 3 patch ant.	Pattern	2.4 - 2.5 1 band	-30°, 30°	12	98 × 90	6.5	NA	Genetic algorithm
[39]	Array 10 × 10 patch	Pattern	1.9 - 2.1 1 band	-10°, 10°	100	345 × 345	14.7	NA	No
[6]	Yagi – Uda antenna	Pattern	3.32 - 3.62 1 band	-17°, 14°	8	100 × 100	7	NA	No
[40]	5 circular patch ant.	Pattern	2.36 - 2.39 1 band	-22°, 22°	4	120 × 120	7.5	76	No
[41]	Driven and passive patch ant.	Pattern	4.9 - 5.1 1 band	-40°, 40°	6	60 × 67	8	81	RA optimization
[42]	Monopole	Pattern	3 – 6 1 band	Simple control omni / endfire	4	38 × 42	1.8	NA	No
[43]	Rectangular patch ant.	Pattern	2.45 1 band	Simple control up / down / left / right	8	100 × 95.5	7.12	NA	No
[44]	Closed ring resonator	Pattern	1.74 - 4.76 3 & 4 bands	Simple control omni - direction / bi - direction	5	29 × 34	1.85	NA	No
Our work	Hybrid antenna Bow-Tie and horn	Pattern	26 - 29.5 Certain freq. according required ML model	-78.1°, 78.1°	3	14.3 × 21.6	8.22	93.2	MLP

compared. This is meant to make it easier for readers to choose the reconfigurable antennas that are most suited to their applications.

It can be seen from the previous Table 3 that our proposed antenna is the best of modern antennas in terms of many features, the most important of which is that our antenna does not operate at multiple frequencies at the same time,

thus causing interference between our frequencies and other frequencies in the work environment, but rather it works at the required frequency only according to the required ML model and then starts the reconfigurability operation using PIN diodes. The coverage angle of the antenna ranges from -78.1° to 78.1°, which is a wide and large range and is considered the largest range of any antenna compared to it. This

antenna is also distinguished by its ease of manufacturing, as there are only three PIN diodes, which is not a large number as in the rest of the antennas, and this antenna has higher gain and radiation efficiency compared to the rest of the antennas in the Table 3. For the pattern-reconfigurable antenna designs, it should be highlighted that our antenna design provides great performance, it is thus a good contender for both present-day and upcoming wireless applications, it shows that the suggested antenna design is a useful design approach for wireless application devices with size limitations.

## VI. CONCLUSION

In this study, a ML-based soft calculation framework is modeled utilizing a full-wave 3D EM analysis platform in order to compute the resonance frequency of the RHBD antenna using ML. A collection of input-output data pairs using the MGSA-PSO algorithm are used to train the network. The simulations with various geometric dimensions define a database including the resonance frequency of 180 RHBD antennas. The database is separated into datasets #162 and #18, respectively, for training and testing the model. As a consequence, the most accurate resonant frequency estimation was performed using the suggested ML model, making it a practical and cost-effective substitute for expensive simulations and testing. This study was not limited to the possibility of changing the resonance frequency only, but three PIN diodes are placed in the middle gaps of the reflectors located at the back of the antenna, and by changing the state of these PIN diodes, it can be noticed that they have a significant and direct effect on the radiation pattern, as they are able to change the beamwidth from  $10.7^\circ$  to  $156.2^\circ$ . The proposed antenna can be used in beamwidth control enables the antenna system to respond to spatial user variations in a dynamical manner, which is prominent for many 5G use case scenarios in high mobility environments.

## ACKNOWLEDGMENT

The author would like to thank the National Telecommunication Regulatory Authority (NTRA), Egypt, for their support.

## REFERENCES

- [1] T. E. Bogale and L. B. Le, "Massive MIMO and mmWave for 5G wireless HetNet: Potential benefits and challenges," *IEEE Veh. Technol. Mag.*, vol. 11, no. 1, pp. 64–75, Feb. 2016.
- [2] Y. J. Guo, P.-Y. Qin, S.-L. Chen, W. Lin, and R. W. Ziolkowski, "Advances in reconfigurable antenna systems facilitated by innovative technologies," *IEEE Access*, vol. 6, pp. 5780–5794, 2018.
- [3] J. Hu, S. Lin, and F. Dai, "Pattern reconfigurable antenna based on morphing bistable composite laminates," *IEEE Trans. Antennas Propag.*, vol. 65, no. 5, pp. 2196–2207, May 2017.
- [4] N. H. Chamok, M. H. Yılmaz, A. Arslan, and M. Ali, "High-gain pattern reconfigurable MIMO antenna array for wireless handheld terminals," *IEEE Trans. Antennas Propag.*, vol. 64, no. 10, pp. 4306–4315, Oct. 2016.
- [5] A. M. Montaser, "Reconfigurable antenna for RFID reader and notched UWB applications using DTO algorithm," *Prog. Electromagn. Res. C*, vol. 47, pp. 65–74, 2014.
- [6] W.-Q. Deng, X.-S. Yang, C.-S. Shen, J. Zhao, and B.-Z. Wang, "A dual-polarized pattern reconfigurable Yagi patch antenna for microbase stations," *IEEE Trans. Antennas Propag.*, vol. 65, no. 10, pp. 5095–5102, Oct. 2017.
- [7] D. Rodrigo, J. Romeu, B. A. Cetiner, and L. Jofre, "Pixel reconfigurable antennas: Towards low-complexity full reconfiguration," in *Proc. 10th Eur. Conf. Antennas Propag. (EuCAP)*, Davos, Switzerland, Apr. 2016, pp. 1–5.
- [8] M. W. Young, S. Yong, and J. T. Bernhard, "A miniaturized frequency reconfigurable antenna with single bias, dual varactor tuning," *IEEE Trans. Antennas Propag.*, vol. 63, no. 3, pp. 946–951, Mar. 2015.
- [9] S. V. Hum and J. Perruisseau-Carrier, "Reconfigurable reflectarrays and array lenses for dynamic antenna beam control: A review," *IEEE Trans. Antennas Propag.*, vol. 62, no. 1, pp. 183–198, Jan. 2014.
- [10] B. A. Cetiner, H. Jafarkhani, J.-Y. Qian, H. J. Yoo, A. Grau, and F. D. Flaviis, "Multifunctional reconfigurable MEMS integrated antennas for adaptive MIMO systems," *IEEE Commun. Mag.*, vol. 42, no. 12, pp. 62–70, Dec. 2004.
- [11] Y. Pan, Y. Hou, M. Li, R. M. Gerdes, K. Zeng, M. A. Towfiq, and B. A. Cetiner, "Message integrity protection over wireless channel: Countering signal cancellation via channel randomization," *IEEE Trans. Depend. Sec. Comput.*, vol. 17, no. 1, pp. 106–120, Jan. 2020.
- [12] W. A. Awan, A. Zaidi, N. Hussain, A. Iqbal, and A. Baghdad, "Stub loaded, low profile UWB antenna with independently controllable notch-bands," *Microw. Opt. Technol. Lett.*, vol. 61, no. 11, pp. 2447–2454, Nov. 2019.
- [13] A. Iftikhar, S. M. Asif, J. M. Parrow, J. W. Allen, M. S. Allen, A. Fida, and B. D. Braaten, "Changing the operation of small geometrically complex EBG-based antennas with micron-sized particles that respond to magnetostatic fields," *IEEE Access*, vol. 8, pp. 78956–78964, 2020.
- [14] A. Iftikhar, J. Parrow, S. Asif, A. Fida, J. Allen, M. Allen, B. Braaten, and D. Anagnostou, "Characterization of novel structures consisting of micron-sized conductive particles that respond to static magnetic field lines for 4G/5G (sub-6 GHz) reconfigurable antennas," *Electronics*, vol. 9, no. 6, p. 903, May 2020.
- [15] A. Ahmad, F. Arshad, S. I. Naqvi, Y. Amin, H. Tenhunen, and J. Loo, "Flexible and compact spiral-shaped frequency reconfigurable antenna for wireless applications," *IETE J. Res.*, vol. 66, no. 1, pp. 22–29, Jan. 2020.
- [16] R. L. Haupt and M. Lanagan, "Reconfigurable antennas," *IEEE Antennas Propag. Mag.*, vol. 55, no. 1, pp. 49–61, Feb. 2013.
- [17] M. K. A. Rahim, M. R. Hamid, N. A. Samsuri, N. A. Murad, M. F. M. Yusoff, and H. A. Majid, "Frequency reconfigurable antenna for future wireless communication system," in *Proc. 46th Eur. Microw. Conf. (EuMC)*, London, U.K., Oct. 2016, pp. 965–970.
- [18] E. A. Abbas, A. T. Mobashsher, and A. Abbosh, "Polarization reconfigurable antenna for 5G cellular networks operating at millimeter waves," in *Proc. IEEE Asia Pacific Microw. Conf. (APMC)*, Kuala Lumpur, Malaysia, Nov. 2017, pp. 772–774.
- [19] J. Costantine, R. Kanj, Z. Ghorayeb, T. Al Bahar, Y. Itani, Y. Tawk, and C. G. Christodoulou, "A radiation pattern reconfigurable antenna for WLAN access," in *Proc. United States Nat. Committee URSI Nat. Radio Sci. Meeting (USNC-URSI NRSM)*, Boulder, CO, USA, Jan. 2016, pp. 1–2.
- [20] S. K. Patel, J. Surve, V. Katkar, and J. Parmar, "Machine learning assisted metamaterial-based reconfigurable antenna for low-cost portable electronic devices," *Sci. Rep.*, vol. 12, no. 1, Jul. 2022, Art. no. 12354.
- [21] A. Belen, F. Günes, M. Palandoken, O. Tari, M. A. Belen, and P. Mahouti, "3D EM data driven surrogate based design optimization of traveling wave antennas for beam scanning in X-band: An application example," *Wireless Netw.*, vol. 28, pp. 1827–1834, Mar. 2022.
- [22] F. Zardi, P. Nayeri, P. Rocca, and R. Haupt, "Artificial intelligence for adaptive and reconfigurable antenna arrays: A review," *IEEE Antennas Propag. Mag.*, vol. 63, no. 3, pp. 28–38, Jun. 2021.
- [23] A. M. Montaser and K. R. Mahmoud, "Design of intelligence reflector metasurface using deep learning neural network for 6G adaptive beamforming," *IEEE Access*, vol. 10, pp. 117900–117913, 2022.
- [24] J. Noh, Y.-H. Nam, S.-G. Lee, I.-G. Lee, Y. Kim, J.-H. Lee, and J. Rho, "Reconfigurable reflective metasurface reinforced by optimizing mutual coupling based on a deep neural network," *Photon. Nanostruct., Fundam. Appl.*, vol. 52, Dec. 2022, Art. no. 101071.
- [25] H. M. El Misilmani, T. Naous, and S. K. Al Khatib, "A review on the design and optimization of antennas using machine learning algorithms and techniques," *Int. J. RF Microw. Comput.-Aided Eng.*, vol. 30, no. 10, pp. 1–28, Oct. 2020.
- [26] A. M. Montaser and K. R. Mahmoud, "Deep learning based antenna design and beam-steering capabilities for millimeter-wave applications," *IEEE Access*, vol. 9, pp. 145583–145591, 2021.
- [27] K. R. Mahmoud and A. M. Montaser, "Machine-learning-based beam steering in a hybrid plasmonic nano-antenna array," *J. Opt. Soc. Amer. B, Opt. Phys.*, vol. 39, no. 8, pp. 2149–2163, 2022.



- [28] K. R. Mahmoud and A. M. Montaser, "Design of multiresonance flexible antenna array applicator for breast cancer hyperthermia treatment," *IEEE Access*, vol. 10, pp. 93338–93352, 2022.
- [29] J. H. Kim and S. W. Choi, "A deep learning-based approach for radiation pattern synthesis of an array antenna," *IEEE Access*, vol. 8, pp. 226059–226063, 2020.
- [30] I. Develi, "Application of multilayer perceptron networks to laser diode nonlinearity determination for radio-over-fibre mobile communications," *Microw. Opt. Technol. Lett.*, vol. 42, no. 5, pp. 425–427, 2004.
- [31] S. Haykin, *Neural Networks: A Comprehensive Foundation*. New York, NY, USA: Macmillan, 1994.
- [32] J.-S. R. Jang, "Self-learning fuzzy controllers based on temporal back-propagation," *IEEE Trans. Neural Netw.*, vol. 3, no. 5, pp. 714–723, Sep. 1992.
- [33] K. R. Mahmoud and A. M. Montaser, "Synthesis of multi-polarised upside conical frustum array antenna for 5G mm-Wave base station at 28/38 GHz," *IET Microw., Antennas Propag.*, vol. 12, no. 9, pp. 1559–1569, Jul. 2018.
- [34] K. R. Mahmoud and A. M. Montaser, "Performance of tri-band multi-polarized array antenna for 5G mobile base station adopting polarization and directivity control," *IEEE Access*, vol. 6, pp. 8682–8694, 2018.
- [35] *Computer Simulation Technology Microwave Studio (CST MWS)*. Accessed: 2022. [Online]. Available: <https://www.3ds.com/products-services/simulia/products/cst-studio-suite/>
- [36] A. Akdagli, A. Toktas, A. Kayabasi, and I. Develi, "An application of artificial neural network to compute the resonant frequency of E-shaped compact microstrip antennas," *J. Electr. Eng.*, vol. 64, no. 5, pp. 317–322, Sep. 2013.
- [37] V. Allam, B. T. P. Madhav, D. Gopi, and K. P. Vinay, "NodeMCU controlled tortoise-shaped bandwidth reconfigurable antenna for 4G and 5G applications," *J. Instrum.*, vol. 16, no. 12, Dec. 2021, Art. no. P12004.
- [38] Z. Li, E. Ahmed, A. M. Eltawil, and B. A. Cetiner, "A beam-steering reconfigurable antenna for WLAN applications," *IEEE Trans. Antennas Propag.*, vol. 63, no. 1, pp. 24–32, Jan. 2015.
- [39] T. Debogovic and J. Perruisseau-Carrier, "Array-fed partially reflective surface antenna with independent scanning and beamwidth dynamic control," *IEEE Trans. Antennas Propag.*, vol. 62, no. 1, pp. 446–449, Jan. 2014.
- [40] M. Jusoh, T. Aboufoul, T. Sabapathy, A. Alomainy, and M. R. Kamarudin, "Pattern-reconfigurable microstrip patch antenna with multidirectional beam for WiMAX application," *IEEE Antennas Wireless Propag. Lett.*, vol. 13, pp. 860–863, 2014.
- [41] M. A. Towfiq, I. Bahceci, S. Blanch, J. Romeu, L. Jofre, and B. A. Cetiner, "A reconfigurable antenna with beam steering and beamwidth variability for wireless communications," *IEEE Trans. Antennas Propag.*, vol. 66, no. 10, pp. 5052–5063, Oct. 2018.
- [42] T. Aboufoul, C. Parini, X. Chen, and A. Alomainy, "Pattern-reconfigurable planar circular ultra-wideband monopole antenna," *IEEE Trans. Antennas Propag.*, vol. 61, no. 10, pp. 4973–4980, Oct. 2013.
- [43] Z.-L. Lu, X.-X. Yang, and G.-N. Tan, "A multidirectional pattern-reconfigurable patch antenna with CSRR on the ground," *IEEE Antennas Wireless Propag. Lett.*, vol. 16, pp. 416–419, 2017.
- [44] G. Singh, B. K. Kanaujia, V. K. Pandey, D. Gangwar, and S. Kumar, "Pattern and frequency reconfigurable antenna with diode loaded ELC resonator," *Int. J. Microw. Wireless Technol.*, vol. 12, no. 2, pp. 163–175, Mar. 2020.



**AHMED M. MONTASER** received the B.S. and M.S. degrees in communications and electronics engineering from South Valley University, Aswan, Egypt, in 2003 and 2009, respectively, and the Ph.D. degree from Mansoura University, Egypt, in 2013. He is currently an Associate Professor with the Department of Communication and Electronics, Faculty of Technology and Education, Sohag University, Sohag, Egypt. He has authored more than 35 articles on microwave-based smart antenna, conformal array devices, and mmWave antennas. He has served as an editor/reviewer for many international journals. His current research interests include microwave applications in biomedical, especially in breast and brain cancer, hyperthermia, and using millimeter wave for cancer detection.

•••